Philosophical Magazine,
Vol. 00, No. 00, DD Month 200x, 1–9

First-principles investigation of superconductivity in the body-centered tetragonal $LaRu_2P_2$

Ertuğrul Karaca[1], S. Karadağ[1], H. M. Tütüncü*[1,2], G. P. Srivastava[3], Ş. Uğur[4]

[1]Sakarya Üniversitesi, Fen-Edebiyat Fakültesi, Fizik Bölümü, 54187, Adapazarı, Turkey

[2]Sakarya Üniversitesi, Biyomedikal, Manyetik ve Yarıiletken Malzemeler Araştırma Merkezi (BIMAYAM), 54187, Adapazarı, Turkey

[3]School of Physics, University of Exeter, Stocker Road, Exeter EX4 4QL, UK

[4]Gazi Üniversitesi,Fen Fakültesi, Fizik Bölümü ,Ankara, Turkey

(Received 00 Month 200x; in final form 00 Month 200x)

We have investigated the ground state and electronic properties of $LaRu_2P_2$ in the $ThCr_2Si_2$ structure using a generalized gradient approximation of the density functional theory and the *ab initio* pseudopotential method. We find that the calculated electronic properties of $LaRu_2P_2$ exhibit three-dimensional rather than two-dimensional characteristics in spite of the apparent two dimensionality in its atomic structure. An interesting feature of the phonon dispersion curves is the phonon anomaly in the lowest transverse acoustic branch as well as the longitudinal acoustic branch. We have shown that these phonon anomalies give rise to large electron-phonon interaction, as is evident from the calculated Eliashberg spectral function $\alpha^2F(\omega)$. By integrating this spectral function, the value of average electron-phonon coupling parameter is calculated to be 0.85, from which the superconducting critical temperature is estimated to be 3.74 K, in gratifying accord with its experimental value of 4.0 K.

1 Introduction

$ThCr_2Si_2$-type AM_2X_2 compounds (A: an alkaline earth or a lanthanide element; M: a transition metal; X: Si, P, Ge, or As) have attracted considerable interest in recent years. These compounds exhibit a great variety of intriguing physical properties, such as low temperature superconductivity [1–10], high temperature superconductivity either under pressure [11–13] or after doping [14–18], and different magnetic structures [19]. Furthermore, some of the $ThCr_2Si_2$-type compounds show complex anisotropic character [20] which may cause to first or second order phase transition under pressure [13, 21]. In particular, lanthanum ruthenium phosphide $LaRu_2P_2$ was found to exhibit superconductivity with the transition temperature of 4.0 K more that 25 years ago [2]. This material is of special interest with respect to superconductivity because, in contrast to its arsenic counterparts, no magnetic order is available to possibly weaken or interfere with superconducting state. Some experimental works [22–25] have been done on the electronic and superconducting properties of $LaRu_2P_2$. Ying and co-workers [23] have investigated the anisotropy of upper and lower critic fields. Both upper and lower critical fields indicate the isotropic superconductivity in this material which is similar to the iron-based superconductors. The isotropic superconductivity [23] reveals the three-dimensional of its Fermi surface topology. Following this experimental work [23], Moll and co-workers [24] have studied the angular de Hass-van Alphen oscillations using magnetic torque in pulsed magnetic fields up to 60 T. In this experimental work [24], the observed oscillation frequencies are in good accordance with the geometry of the calculated Fermi surface. After this experimental work, the experimental study of Razzoli *et. al.* [25] shows that the origin of the superconducting phase in $LaRu_2P_2$ differs from the one in the 122 Fe pnictides and more conventional in the sense that it arises from a Fermi-liquid-like normal state. On the theoretical side, the density functional theory [24, 25] has been used to

* Corresponding author. Email: t utuncu@sakarya.edu.tr

investigate the electronic properties of $LaRu_2P_2$. These theoretical works state that the electronic structure of $LaRu_2P_2$ around the Fermi level is quite three dimensional, and by no means quasi two dimensional.

Although considerable progress has been made to investigate the electronic properties of $LaRu_2P_2$, no experimental or theoretical works have been performed to investigate the vibrational properties of this material. Such a study is very desirable, as a number of interesting properties of solids are governed by electron-phonon interaction. We have performed a first-principles theoretical investigation of the ground state atomic structural, electronic structural, and phonon structural properties of $LaRu_2P_2$ in the body-centered tetragonal $ThCr_2Si_2$ structure. Using the results of these investigations, the linear response method [26] and the Migdal-Eliashberg approach [27–30] have been utilized to calculate the Eliashberg spectral function and the average electron-phonon coupling parameter. In particular, the role of phonon anomalies in determining the electron-phonon coupling parameter has been highlighted. The calculated superconducting parameters are compared with the experimental values reported by Moll and co-workers [24].

2 Theory

The computer package QUANTUM ESPRESSO [26] has been used to investigate the structural, electronic, vibrational and electron-phonon interaction properties of $LaRu_2P_2$. This package performs density functional calculations of material properties using pseudopotentials and the plane wave basis set. The electronic exchange-correlation energy is included using the Perdew-Burke-Ernzerhof expression [31] within the generalized gradient density functional approximation (GGA). The interaction of the valence electrons with the ionic cores are represented with ultrasoft pseudopotentials [32, 33]. The maximum plane wave cutoff energy is chosen to be 60 Ry while self-consistent solutions of the Kohn-Sham equations [34] are determined by employing a set of Monkhorst-Pack special [35] $\boldsymbol{k}$ points within the Brillouin zone. Integration over the Brillouin zone (BZ) for total-energy calculations has been made using the $8\times8\times8$ zone-centred grid, producing 59 $\boldsymbol{k}$ points in the irreducible part of the BZ (IBZ). The self-consistent electronic structure calculations are performed out by using the $24\times24\times24$ zone-centred grid, producing 1063 $\boldsymbol{k}$ points in the IBZ.

Phonon dispersion relations have been studied using the *ab initio* linear response method [26], which permits the calculation of the dynamical matrix at arbitrary $\boldsymbol{q}$ vectors without the use of supercells. Using the eigenfrequencies and eigenvectors of lattice vibrations a static linear response of the valence electrons is considered in terms of the variation of the external potential corresponding to periodic displacements of the atoms in the unit-cell. The screening of the electronic system in response to the displacement of the atoms has been determined in a self consistent manner. Integration up to the Fermi surface has been made by employing the smearing technique with the broadening parameter $\sigma = 0.02$ Ry. The numerical integration of the Brillouin zone for phonon calculations has been performed using the $8\times8\times8$ Monkhorst-Pack $\boldsymbol{k}$-point sampling. The dynamical matrices have been calculated on a $4\times4\times4$ $\boldsymbol{q}$-point mesh, and a Fourier interpolation has been done to determine the full phonon spectrum and the vibrational density of states. The calculation of the electron-phonon coupling follows the steps described in our previous works [36–38]. Fermi-surface sampling for the evaluation of the electron-phonon matrix elements has been made using $24\times24\times24$ $\boldsymbol{k}$-mesh with a Gaussian width 0.02 Ry. The phonon density of states and the Eliashberg spectral function are also determined using this $\boldsymbol{k}$-mesh.

3 Results

3.1 *Structural and Electronic Properties*

The $ThCr_2Si_2$ crystal structure of $LaRu_2P_2$ is shown in Fig. 1. This is a body-centered tetragonal structure with space group I4/mmm. The primitive unit cell contains one La atom at the 2a (0, 0, 0) position, two Ru atoms at 4d (0, 1/2, 1/4) and two P atoms at 4e (0, 0, z). Here z shows the internal parameter which governs the relative position of P within the unit cell. This crystal structure of $LaRu_2P_2$ is primarily formed by layers of edge-sharing RuP_4 tetrahedra in the x-y plane separated by La atoms. The α, β and γ angles are good indicators of distortion in RuP_4 tetrahedra. The La sheets behave as the so-called charge reservoir layers, which procures electron transfer from La layers to $[Ru_2P_2]$ layers. Thus, neighboring La-$[Ru_2P_2]$ layers are coupled due to their ionic interactions. In addition to this ionic bonding, covalent Ru-P bonds exist between the atoms inside the conducting $[Ru_2P_2]$ layers. Furthermore, the bonding in this compound includes a metallic character, mainly due to the d electrons of Ru atoms. Consequently, the overall bonding situation in $LaRu_2P_2$ can be described as an interplay between covalent, metallic and ionic interactions.

As the first step of our *ab initio* work, total energy calculations are made to obtain the equilibrium structural parameters for $LaRu_2P_2$. Then, around the region of the total energy minimum, the bulk modulus, the pressure coefficient $B^{'}$ and the equilibrium volume are determined by fitting numerical data to Murnaghan's equation of state [39]. The calculated equilibrium lattice constants (a and c), the internal parameter (z), the bulk modulus B, the pressure coefficient $B^{'}$, the closest Ru-P distance (d_{Ru-P}), and the bond angles (α, β and γ) are given and compared with available experimental [2, 22, 24] and theoretical results [25] in Tab. 1. In general, the calculated lattice parameters (a and c) and the bond angles (α, β and γ) are in excellent accordance with their experimental values [2,22,24] . The deviation of a and c from their recent experimental values [24] of 4.025 $\AA$ and 10.662 $\AA$ is 1.0% and 0.4%, respectively, while the calculated value of internal parameter is essentially equal to its experimental value of 0.359 [2].

Fig. 2(a) displays the calculated energy band structure of $LaRu_2P_2$ along selected high-symmetry directions within the body-centered tetragonal first Brillouin zone, while the total and partial electronic density of states (DOS) are illustrated in Fig. 2 (b). We find the overall band profiles to be very similar to previous theoretical results [24, 25]. The energy bands close to the Fermi level display considerable dispersion along the Γ-Z direction, indicating a three dimensional nature of the electronic structure. While occupied and unoccupied bands are well separated from each other only along the X-P symmetry direction, the metallic character of this material is confirmed as at least one band crosses the Fermi level along Γ-G1, Γ-Z, Γ-P, and Γ-N directions. The lowest two bands arise from the s electrons of P atoms. These 's' bands are well separated by a gap of 4 eV from the main valence band region from -6.7 eV to the Fermi level. These bands form a peak at about -11.4 eV in the electronic DOS. Ru 4d, Ru 5p and La 6p make lesser contributions to this strong peak. For energy window from -6 to -3 eV, there is a high degree of hybridization of Ru d states with P p states, which is the evidence for a strong covalent interaction between Ru and P atoms. The covalent bond between these atoms can be related to the similarity of their electronegativities. The DOS curve reveals two peaks with energies -1.9 and -1.2 eV in energy window from -3.0 to -1.0 eV. Ru 4d orbital states contribute to these two peaks strongly while lesser contributions to these peaks arise from P 3p, La 5d and Ru 5p states.

Since electrons near the Fermi level form the superconducting properties of solids, it is mandatory to explore their nature. From -1.0 eV to the Fermi level, the DOS are strongly dominated by Ru 4d states. Moreover, the La 5d, P 3p and Ru 5p states also exist in this energy region. The DOS features above the Fermi level are mainly composed of La 5d, Ru 4d, P 3p and Ru 5p orbitals. The value of DOS at the Fermi level ($N(E_F)$) amounts to be 2.38 states/eV, which compares well the previous GGA value of 2.46 states/eV in the work of Razzoli *et al* [24]. The contributions from La, Ru and P atoms to $N(E_F)$ are approximately 29%, 48%, and 23%, respectively. Ru 4d, La 5d and P 3p states alone contribute 41%, 26% and 19% to $N(E_F)$, respectively. Thus, we conclude that the metallic properties of $LaRu_2P_2$ are mainly formed by the d states coming from the transition metal Ru atoms. The huge contribution from Ru 4d states to $N(E_F)$ affects the superconducting properties of this material strongly, since according to the McMillan-Hopfield expression, the electron-phonon coupling constant (λ) can be given in the following form [29, 30]

$$\lambda = \frac{N(E_F) < I^2 >}{M < \omega^2 >}, \tag{1}$$

where M is the average atomic mass, $< \omega^2 >$ shows the average of squared phonon frequencies, and $< I^2 >$ represents the Fermi surface average of squared electron-phonon coupling interaction. According to the above equation, the value of the electron-phonon coupling constant (λ) increases linearly with $N(E_F)$.

3.2 *Phonons and Superconductivity*

All of the 12 zone-center phonon modes in $LaRu_2P_2$ can be categorized by the irreducible representation of the point group D_{4h} (4/mmm). As prescribed by group theory, the symmetries of the optical phonon modes can be stated as:

$$\Gamma = 2E_u + 2A_u + B_{1g} + 2E_g + A_{1g}$$

where u and g modes are infrared (IR) and Raman active respectively. The frequencies of zone center phonon modes are presented together with their electron-phonon coupling parameters and their eigen characters in Tab. 2. The one-dimensional A and B modes correspond to the vibrations of related atoms along the z-direction, while the doubly degenerate E modes arise from the motion of relevant atoms in the x–y plane. The analysis of Tab. 2 indicates that all zone-center optical phonon modes have negligible electron-phonon coupling parameter. Thus, we can conclude that the zone-center phonon modes do not play a significant role in determining the superconducting properties of $LaRu_2P_2$.

The calculated phonon dispersion curves, and the total and partial phonon density of states (DOS), of $LaRu_2P_2$ are shown in Fig. 3. A few remarkable features of the phonon spectrum can be noted. It splits into a low-frequency band (LFB) (0-7.1 THz) and a high-frequency band (HFB) (9.3-11.70 THz) which are separated from each other by a phonon band gap of 2.2 THz. The LFB is formed by the three acoustic and six optical branches, while the HFB contains the remaining six optical phonon branches. The acoustic and optical branches in the LFB are dispersive along the high symmetry lines, except X-P. There is significant overlap between acoustic and optical phonon branches. The computed transverse acoustic branches (lower-lying TA_1 and upper-lying TA_2) and the longitudinal branch behave normally in the long-wave limit with steep slopes. However, as can be seen from Fig. 3(a), for most part along the Γ-G1-Z direction, the LA branch lies below the TA branches. This represents a pronounced anomaly in the dispersion of the LA branch (see the red solid line in Fig. 3(a)). Furthermore, the lower-lying transverse acoustic (TA_1) branch (see the blue solid line in Fig. 3(a)) starts to show a negative dispersion (phonon anomaly) close the zone boundary N along the Γ-N symmetry direction. The correlation between phonon anomalies and superconductivity has been known since the late 1960s. Countless studies [36, 40–51] have indicated that the largest contribution to electron-phonon mass enhancement parameter (*i.e.* average electron-phonon coupling parameter) comes from phonon branches which show anomaly. Finally, the high frequency optical branches in the HFB are neither pure P states or mixed Ru-P modes. Such high frequencies of Ru vibrations indicate rather strong covalent bonding forces between Ru and P atoms.

The nature of the phonon dispersion relations can be understood more overtly by closely examining the total and partial phonon DOS in Fig. 3(b). Eigendisplacements involving all the three atomic species are found for frequencies below 4.0 THz. In particular, the frequency region below 2.0 THz is mainly due to the coupled motion of Ru and P atoms with a lesser contribution from La atoms. However, La vibrations are dominant between 2.0 and 4.0 THz and disappear above 4.0 THz due to the heavy mass of La. In the 4.0-6.0 THz range, the DOS features arise from the vibrations of Ru atoms with a considerable admixture of P vibrations. In the 6.0-7.0 THz range strong Ru-P hybridization exists due to strong covalent bond between these atoms. While P vibrations exist both in LFB as well as HFB, they are certainly dominant above the phonon band gap region which can be linked to the light mass of P.

The first noticeable feature of the phonon dispersion curves for $LaRu_2P_2$ is the softening of the LA branch along the Γ-G1-Z direction. With increased wave numbers along Γ-G1, the LA branch first crosses the upper-lying TA_2 branch and then the lower-lying TA_1 branch. Thus, along this direction, the LA branch acquires a pronounced dip, with frequency lower than the transverse acoustic branches. The dip in the LA branch is found at $\boldsymbol{q} = \frac{2\pi}{a}(0.75, 0.0, 0.0)$ with frequency 0.94 THz. The second noticeable feature of the phonon dispersion curves is the anomaly of the lower-lying TA_1 branch along the Γ-N symmetry direction. These striking phonon anomalies of the LA and TA_1 branches are crucial for superconductivity in $LaRu_2P_2$, because a positive connection between phonon anomalies and electron-phonon interaction is well known [36,40–51]. In order show a positive relationship between the anomalous phonon dispersion and electron-phonon interaction, we have identified the mode-dependent electron-phonon coupling parameter $\lambda_{\mathbf{q},j}$ for acoustic phonon branches. Gripping characteristics are found along two main symmetry directions Γ-G1-Z and Γ-N in Fig. 4. The most outstanding characteristic is that the electron-phonon coupling parameter of LA branch takes it largest value of 0.81 at $\mathbf{q} = \frac{2\pi}{a}(0.75,\ 0.0,\ 0.0)$, where the frequency of this branch has its lowest value of 0.94 THz. This observation is the first evidence for a positive relationship between phonon anomaly and electron-phonon coupling parameter. Secondly, the phonon anomaly of TA$_1$ is found to occur between $\boldsymbol{q} = \frac{2\pi}{a}(0.0, 0.35, \frac{0.35a}{c})$ and the zone boundary of N point. Due to this phonon anomaly, the electron-phonon coupling parameter of this branch increases rapidly beyond $\boldsymbol{q} = \frac{2\pi}{a}(0.0, 0.35, \frac{0.35a}{c})$, reaching its largest value of 1.08 at the N zone-boundary. We can conclude that this is the second evidence for a positive relationship between phonon anomaly and the electron-phonon coupling parameter.

In order to further establish the role of phonons in developing superconductivity in LaRu$_2$P$_2$, we have presented the frequency-dependent Eliashberg function $\alpha^2F(\omega)$ and the frequency-accumulative electron-phonon coupling parameter λ in Fig. 5. A comparison of the Eliashberg spectral function with the phonon density of states in Fig. 3(b) explains that phonon modes in the entire frequency range contribute to the electron-phonon interaction, *albeit* with different amounts. In particular, Ru-related vibrations below 2 THz contribute approximately 48% (0.408) to λ. This result is expected since the states near the Fermi level are primarily contributed by the d electrons of Ru atoms. This large additive contribution from low frequency phonons arise from the factor $\frac{1}{\omega}$ in the expression for λ as given below

$$\lambda = 2\int \frac{\alpha^2F(\omega)}{\omega}\mathrm{d}\omega. \tag{2}$$

The accumulative value electron-phonon coupling parameter is calculated to be 0.85, which reveals that the electron-phonon interaction in LaRu$_2$P$_2$ is of medium strength. This value can be used to calculate the electronic specific-heat coefficient using $\gamma = \gamma_{bs}(1+\lambda)$, which is renormalized by the phonon enhancement factor $(1+\lambda)$ compared to its band structure value ($\gamma_{bs} = \frac{\pi^2 k_B^2 N(E_F)}{3}$). With the calculated value of λ, the superconducting transition temperature (T_c) for LaRu$_2$P$_2$ can be determined from the Allen-Dynes formula [29,30]

$$T_c = \frac{\omega_{\ln}}{1.2}\exp\left(-\frac{1.04(1+\lambda)}{\lambda-\mu^*(1+0.62\lambda)}\right). \tag{3}$$

The above formula links the value of T_c with the electron-phonon coupling parameter λ, the logarithmically averaged frequency ω_{ln} and Coulomb repulsion μ^*. The value of ω_{ln} can be calculated from

$$\omega_{ln} = \exp\left(2\lambda^{-1}\int_0^\infty \frac{\mathrm{d}\omega}{\omega}\alpha^2F(\omega)\ln\omega\right). \tag{4}$$

It is also possible to obtain the value of μ^* from the following modification of the Bennemann-Garland empirical formula [52]

$$\mu^* = \frac{0.26N(E_F)}{(1+N(E_F))}. \tag{5}$$

The calculated parameters related to the superconductivity in LaRu$_2$P$_2$ are compared with previous theoretical and experimental results [2, 24] in Tab. 3. In general, our calculated results compare very well with the experimental values [2, 24]. We note that the calculated value of λ is slightly lower than the experimentally deduced value of 0.98. The calculated value of $T = 3.74$ K is in excellent accordance with the experimental value of 4.0 K [2] and the calculated value of γ = 10.35 mJ mol^{-1} K^{-2} is also in good agreement with the corresponding experimental value of 11.50 mJ mol^{-1} K^{-2} [24].

4 Summary and Conclusion

We have studied the structural, electronic, vibrational and electron-phonon interaction properties of $LaRu_2P_2$ adopting in the body-centered tetragonal $ThCr_2Si_2$ type of crystal structure. The calculated structural parameters are in close agreement with their experimental values. The electronic bands near the Fermi level exhibit a considerable dispersion along the c-axis, indicating that this compound is a three-dimensional metal in spite of the apparent two dimensionality in its atomic structure. From the analysis of the total and partial electronic density of states, we have observed that the states around the Fermi level are contributed by the states originating from Ru atoms, confirming their active role in determining the electronic and superconducting properties of this compound.

Using our calculated lattice constant and electronic structure, phonons in $LaRu_2P_2$ has been studied by employing a linear response approach based on density functional perturbation theory. This compound is dynamically stable, as no instabilities in the phonon dispersion relations have been found. The most impressive features in the phonon spectrum of this material are the phonon anomalies of the LA branch and the lower-lying TA_1 branch along the Γ-G1-Z and Γ-N symmetry directions. We have shown that these phonon anomalies make large contributions to the accumulated electron-phonon coupling parameter.

The Eliashberg spectral function has been calculated using the phonon spectrum and the electron-phonon matrix elements. A critical evaluation of this function suggests that the low-frequency acoustic phonons are more involved in the process of scattering of electrons than the optical phonon modes. From the integration of the calculated Eliashberg function, the value of accumulated electron-phonon coupling constant λ is found to be 0.85, suggesting that $LaRu_2P_2$ is a phonon-mediated superconductor with medium electron-phonon coupling strength. Ru-related vibrations make a large contribution to the electron-coupling parameter due to considerable presence of the Ru d states near the Fermi level. Finally, the value of the electronic specific heat coefficient is calculated to be 10.5 mJ mol^{-1} K^{-2}, which is in good accordance with the experimentally deduced value of 11.50 mJ mol^{-1} K^{-2}.

ACKNOWLEDGMENTS

This work was supported by the Scientific and Technical Research Council of Turkey (TÜBİTAK) (Project Number MFAG-114F192). Some of the calculations for this project were carried out using the computing facilities on the Intel Nehalem (i7) cluster (ceres) in the School of Physics, University of Exeter, United Kingdom.

References

[1] G.W. Hull, J.H. Wernick, T.H. Geballe, J.V. Waszczak, J.E. Bernardini, Superconductivity in the ternary intermetallic s $YbPd_2Ge_2$, $LaPd_2Ge_2$, and $LaPt_2Ge_2$, Phys. Rev. B 24 (1981), pp. 6715–6718.

[2] W. Jeitschko, R. Glaum and L. Boonk, Superconducting $LaRu_2P_2$ and other alkaline earth and rare earth metal ruthenium and osmium phosphides and arsenides with $ThCr_2Si_2$ structure, Journal of Solid State Chemistry 69 (1987), pp. 93–100.

[3] F. Ronning, N. Kurita, E. D. Bauer, B. L. Scott, T. Park, T. Klimczuk, R. Movshovich, and J. D. Thompson,The first order phase transition and superconductivity in $BaNi_2As_2$ single crystals, J. Phys.: Condens. Matter 20 (2008), pp. 342203-1–342203-4.

[4] H. Fujii and A. Sato, Superconductivity in $SrPd_2Ge_2$, Phys. Rev. B 79 (2009), pp. 224522-1–224522-5.

[5] N. Berry, C. Capan, G. Seyfarth, A. D. Bianchi, J. Ziller, and Z. Fisk, Superconductivity without Fe or Ni in the phosphides $BaIr_2P_2$ and $BaRh_2P_2$, Phys. Rev. B 79 (2009), pp. 180502-1–180502-4 (R).

[6] Y. Tomioka, S. Ishida, M. Nakajima, T. Ito, H. Kito, A. Iyo, H. Eisaki, and S. Uchida, Three-dimensional nature of normal and superconducting states in $BaNi_2P_2$ single crystals with the $ThCr_2Si_2$-type structure, Phys. Rev. B 79 (2009), pp. 132506-1–132506-4.

[7] D. Hirai, T. Takayama, D. Hashizume, R. Higashinaka, A. Yamamoto, A.K. Hiroko, H. Takagi, Superconductivity in 4d and 5d transition metal layered pnictides $BaRh_2P_2$, $BaIr_2P_2$ and $SrIr_2As_2$ Physica C 470 (2010), pp. 296–297.

[8] N. H. Sung, Jong-Soo Rhyee, and B. K. Cho, Superconductivity and anomalous transport in $SrPd_2Ge_2$ single crystals, Phys. Rev. B 83 (2011), pp. 094511-1–094511-6.

[9] T. K. Kim, A. N. Yaresko, V. B. Zabolotnyy, A. A. Kordyuk, D. V. Evtushinsky, N. H. Sung, B. K. Cho, T. Samuely, P. Szabo, J. G. Rodrigo, J. T. Park, D. S. Inosov, P. Samuely, B. Büchner, and S. V. Borisenko, Conventional superconductivity in $SrPd_2Ge_2$, Phys. Rev. B 85 (2012), pp. 014520-1–014520-7.

[10] V. K. Anand, H. Kim, M. A. Tanatar, R. Prozorov, and D. C. Johnston, Superconducting and normal-state properties of APd_2As_2 (A=Ca, Sr, Ba) single crystals, Phys. Rev. B 87 (2013), pp. 224510-1–224510-22.

[11] M. S. Torikachvili, S. L. Budko, N. Ni and P. C. Caneld, Pressure Induced Superconductivity in $CaFe_2As_2$, Phys. Rev. Lett. 101 (2008), pp. 057006-1–057006-4.

[12] C. F. Miclea, M. Nicklas, H. S. Jeevan, D. Kasinathan, Z. Hossain, H. Rosner, P. Gegenwart, C. Geibel, and F. Steglich, Evidence for a reentrant superconducting state in $EuFe_2As_2$ under pressure, Phys. Rev. B 79 (2009), pp. 212509-1–212509-4.

[13] F. Ronning, E. D. Baur and T. Park, Superconductivity and the effects of pressure and structure in single-crystalline $SrNi_2P_2$, Phys. Rev. B 79 (2009), pp. 134507-1–134507-7.
[14] M. Rotter, M. Tegel, and D. Johrendt, Superconductivity at 38 K in the Iron Arsenide $(Ba_{1-x}K_x)Fe_2As_2$, Phys. Rev. Lett. 101 (2008), pp. 107006-1–107006-4.
[15] A. S. Sefat, R. Jin, M. A. McGuire, B. C. Sales, D. J. Singh, and D. Mandrus, Superconductivity at 22 K in Co-Doped $BaFe_2As_2$ Crystals, Phys. Rev. Lett. 101 (2008), pp. 117004-1–117004-4.
[16] H. S. Jeevan, Z. Hossain, D. Kasinathan, H. Rosner, C. Geibel and P. Gegenwart, High-temperature superconductivity in $Eu_{0.5}K_{0.5}Fe_2As_2$, Phys. Rev. B 78 (2008), pp. 092406-1–092406-4.
[17] L. Shan, J. Gong, Yong-Lei Wang, B. Shen, X. Hou, C. Ren, C. Li, Huan Yang, Hai-Hu Wen, S. Li, and P. Dai,Evidence of a Spin Resonance Mode in the Iron-Based Superconductor $Ba_{0.6}K_{0.4}Fe_2As_2$ from Scanning Tunneling Spectroscopy, Phys. Rev. Lett. 108 (2012), pp. 227002-1–227002-5.
[18] D. Hirai, F. V. Rohr and R. J. Cava, Emergence of superconductivity in $BaNi_2(Ge_{1-x}P_x)_2$ at a structural instability, Phys. Rev. B 86 (2012), pp. 100505-1–100505-5.
[19] M. Reehuis, W. Jeitschko, M.H. Moller, P.J. Brown, A Neutron diffraction study of the magnetic structure of $EuCo_2P_2$, J. Phys. Chem. Solids 53 (1992), pp. 687–690.
[20] I. R. Shein and A. L. Ivanovski, Electronic and structural properties of low-temperature superconductors and ternary pnictides ANi_2Pn_2 (A=Sr,Ba and Pn=P,As), Phys. Rev. B 79 (2009), pp. 054510-1–054510-7.
[21] Yu-Zhong Zhang, Hem C. Kandpal, Ingo Opahle, Harald O. Jeschke, and Roser Valent, Microscopic origin of pressure-induced phase transitions in the iron pnictide superconductors AFe_2As_2: An ab initio molecular dynamics study, Phys. Rev. B 80 (2009), pp. 094530-1–094530-6.
[22] R. E. Schaak and R. J. Cava, Boron substitution in ternary metal phosphide superconductors, Materials Research Bulletin, 39 (2004), pp. 1231–1235.
[23] J. J. Ying, Y. J. Yan, R.H. Liu, X. F. Wang, A. F. Wang, M. Zhang, Z. J. Xiang and X. H. Chen, Isotropic superconductivity in $LaRu_2P_2$ with the $ThCr_2Si_2$-type structure, Supercond. Sci. Tecnol. 23 (2010), pp. 115009-1–115009-4.
[24] P. J. W. Moll, J. Kanter, R. D. McDonald, F. Balakirev, P. Blaha, K. Schwarz, Z. Bukowski, N. D. Zhigadlo, S. Katrych, K. Mattenberger, J. Karpinski, and B. Batlogg,Quantum oscillations of the superconductor $LaRu_2P_2$: Comparable mass enhancement $\lambda = 1$ in Ru and Fe phosphides, Phys. Rev. B 84 (2011), pp. 224507-1–224507-5.
[25] E. Razzoli, M. Kobayashi, V. N. Strocov, B. Delley, Z. Bukowski, J. Karpinski, N. C. Plumb, M. Radovic, J. Chang, T. Schmitt, L. Patthey, J. Mesot, and M. Shi, Bulk Electronic Structure of Superconducting $LaRu_2P_2$ Single Crystals Measured by Soft-X-Ray Angle-Resolved Photoemission Spectroscopy, Phys. Rev. Lett. 108 (2012), pp. 257005-1–257005-5.
[26] P. Giannozzi, S. Baroni, N. Bonini, M. Calandra, R. Car, C. Cavazzoni, D. Ceresoli, G. L. Chiarotti, M. Cococcioni, I. Dabo, A.D. Corso, S. de Gironcoli, S. Fabris, G. Fratesi, R. Gebauer, U. Gerstmann, C. Gougoussis, A. Kokalj, M. Lazzeri, L. Martin-Samos, N. Marzari, F. Mauri, R. Mazzarello, S. Paolini, A. Pasquarello, L. Paulatto, C. Sbraccia, S. Scandolo, G. Sclauzero, A.P. Seitsonen, A. Smogunov, P. Umari and R.M. Wentzcovitch, QUANTUM ESPRESSO: a modular and open-source software project for quantum simulations of materials, J. Phys.: Condens. Matter 21 (2009), pp. 395502-1–395502-19.
[27] A. B. Migdal, Interaction between electrons and lattice vibrations in a normal metal, Zh. Eksp. Teor. Fiz. 34 (1958), pp. 996–1001.
[28] G. M. Eliashberg, Interaction between electrons and lattice vibrations in a superconductor, Sov. Phys. JETP. 11 (1960), pp. 696–702.
[29] P. B. Allen,Neutron Spectroscopy of Superconductors, Phys. Rev. B 6 (1972), pp. 2577–2579.
[30] P. B. Allen and R. C. Dynes, Transition temperature of strong-coupled superconductors reanalyzed, Phys. Rev. B 12 (1975), 905–922.
[31] J. P. Perdew, K. Burke, and M. Ernzerhof, Generalized Gradient Approximation Made Simple, Phys. Rev. Lett. 77 (1996), pp. 3865–3868.
[32] D. Vanderbilt, Soft self-consistent pseudopotentials in a generalized eigenvalue formalism, Phys. Rev. B 41 (1990), pp.7892–7895 (R).
[33] A. M. Rappe, K. M. Rabe, E. Kaxiras, and J. D. Joannopoulos, Optimized pseudopotentials, Phys. Rev. B 41 (1990), pp. 1227–1230 (R).
[34] W. Kohn and L. J. Sham, Self-Consistent Equations Including Exchange and Correlation Effects, Phys. Rev. 140 (1965), pp. A1133–A1138.
[35] H. J. Monkhorst and J. D. Pack, Special points for Brillonin-zone integrations, Phys. Rev. B 13 (1976), pp. 5188–5192.
[36] S. Bağcı, S. Duman, H. M. Tütüncü, G. P. Srivastava, Ground state, phonon spectrum, and superconducting properties of the nonoxide perovskite $CdCNi_3$, Phys. Rev. B. 78 (2008), pp. 174504-1–174504-6.
[37] S. Bağcı, H. M. Tütüncü, S. Duman and G. P. Srivastava, Phonons and superconductivity in fcc and dhcp lanthanum, Phys. Rev. B 81 (2010), pp.144507-1–144507-9.
[38] H. M. Tütüncü, S. Bağcı, G. P. Srivastava and A. Akbulut, Electrons, phonons and superconductivity in rocksalt and tungstencarbide phases of CrC, Journal of Physics:Condensed Matter 24 (2012), pp. 455704-1–455704-12.
[39] F.D. Murnaghan, The Compressibility of Media under Extreme Pressures, Proc. Nat. Acad. Sci., 30 (1944), pp.244–247.
[40] M. Wells, M. Pickus, K. Kennedy, and V. Zackay, Superconductivity of Solid Solutions of TaC and NbC, Phys. Rev. Lett. 12 (1964), pp. 536–538.
[41] B. M. Klein and D. A. Papaconstantopoulos, Electron-Phonon Interaction and Superconductivity in Transition Metals and Transition-Metal Carbides, Phys. Rev. Lett. 32 (1974), pp. 1193–1195.
[42] M. Gupta and A. J. Freeman, Direct Correlation of Phonon Anomalies in NbC with Fermi-Surface-Induced Maxima in Generalized Susceptibilities, Phys. Rev. Lett. 37 (1976), pp. 364–367.
[43] W. Kress, P. Roedhammer, H. Bilz, W. D. Teuchert, and A. N. Christensen, Phonon anomalies in transition-metal nitrides: TiN, Phys. Rev. B 17 (1978), pp. 111–113.
[44] P. Roedhammer, W. Reichardt, and F. Holtzberg, Soft-Mode Behavior in the Phonon Dispersion of YS, Phys. Rev. Lett. 40 (1978), pp. 465–468.
[45] M. Gupta, Electronic instability and phonon softening in YS, Phys. Rev. B 20 (1979), pp. 4334–4342.
[46] X. W. Wang, B. N. Harmon, Y. Chen, K.-M. Ho, C. Stassis, and W. Weber, Anomalous lattice dynamics of fcc lanthanum, Phys. Rev. B 33 (1986), pp. 3851–3856.
[47] R. Heid, B. Renker, H. Schober, P. Adelmann, D. Ernst, and K.-P. Bohnen, Phonon spectrum and soft-mode behavior of $MgCNi_3$, Phys. Rev. B 69 (2004), pp. 092511-1–092511-4.
[48] R. Heid, K.-P. Bohnen, B. Renker, T. Wolf, and H. Schober, Ab initio lattice dynamics and electron-phonon coupling in the refractory compounds ZrN and HfN, Phys. Rev. B 71 (2005), pp. 092302-1–092302-4.
[49] E. I. Isaev, S. I. Simak, I. A. Abrikosov, R. Ahuja, Yu. Kh. Vekilov, M. I. Katsnelson, A. I. Lichtenstein and B. Johansson, Phonon related properties of transition metals, their carbides, and nitrides: A first-principles study, J. Appl. Phys. 101 (2007), pp. 123519-1–123519-18.

[50] S. Kuroiwa, A. Q. R. Baron, T. Muranaka, R. Heid, K.-P. Bohnen, and J. Akimitsu, Soft-phonon-driven superconductivity in CaAlSi as seen by inelastic x-ray scattering, Phys. Rev. B 77 (2008), pp. 140503-1–140503-14 (R).
[51] H. M. Tütüncü, H. Y. Uzunok, Ertuğrul Karaca, G. P. Srivastava, S. Özer, and Ş Uğur, Ab initio investigation of BCS-type superconductivity in $LuNi_2B_2C$-type superconductors, Phys. Rev. B 92 (2015), pp. 054510-1–054510-17.
[52] K. Bennemann and J. Garland, in Superconductivity in d- and f-Band Metals, edited by D. H. Douglass (Plenum, New York, 1973), p. 103.

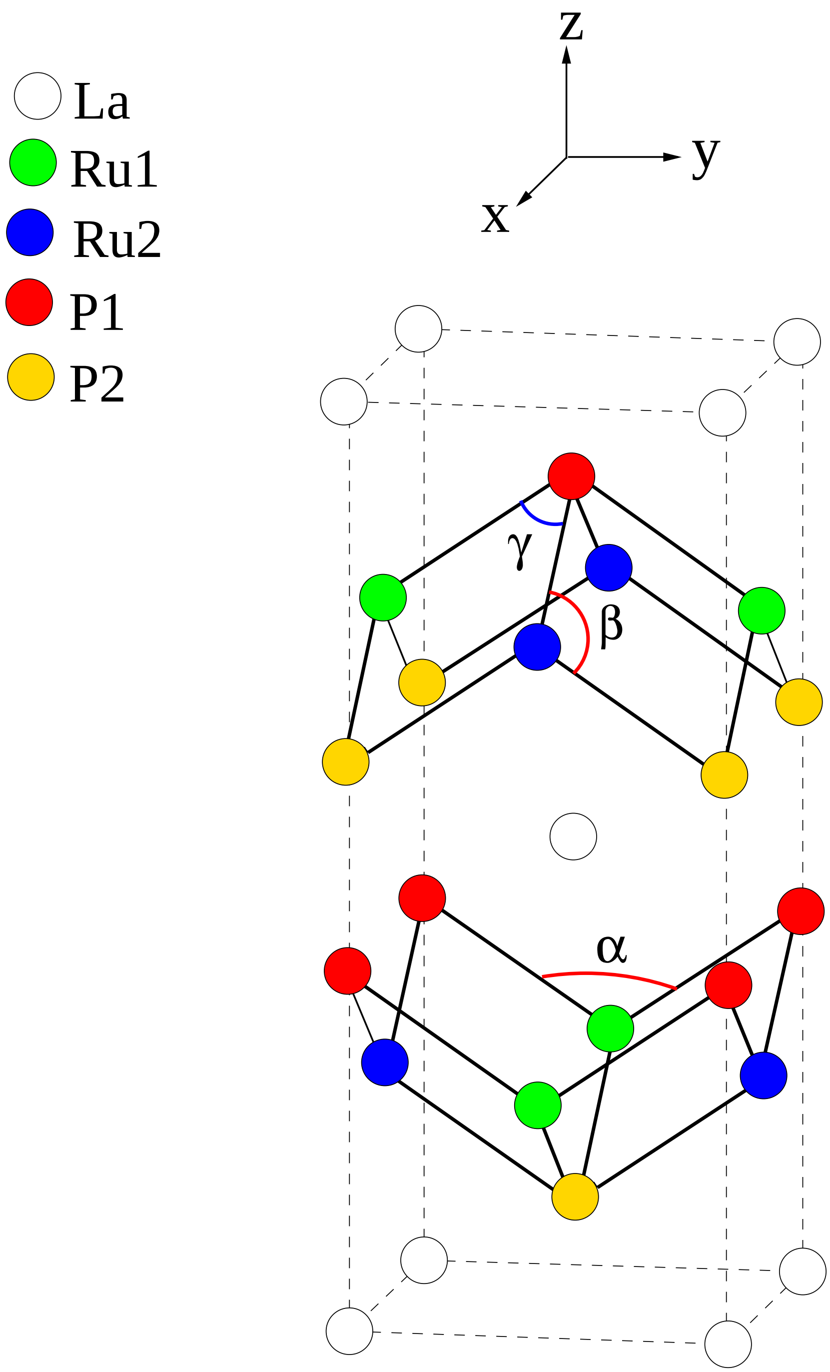

Figure 1. The $ThCr_2Si_2$ structure of $LaRu_2P_2$ showing P-Ru_2-P-type layers and La ion sheets alternatively stacked along the c-axis. The α, β and γ angles are good markers of distortion in the RuP_4 tetrahedron.

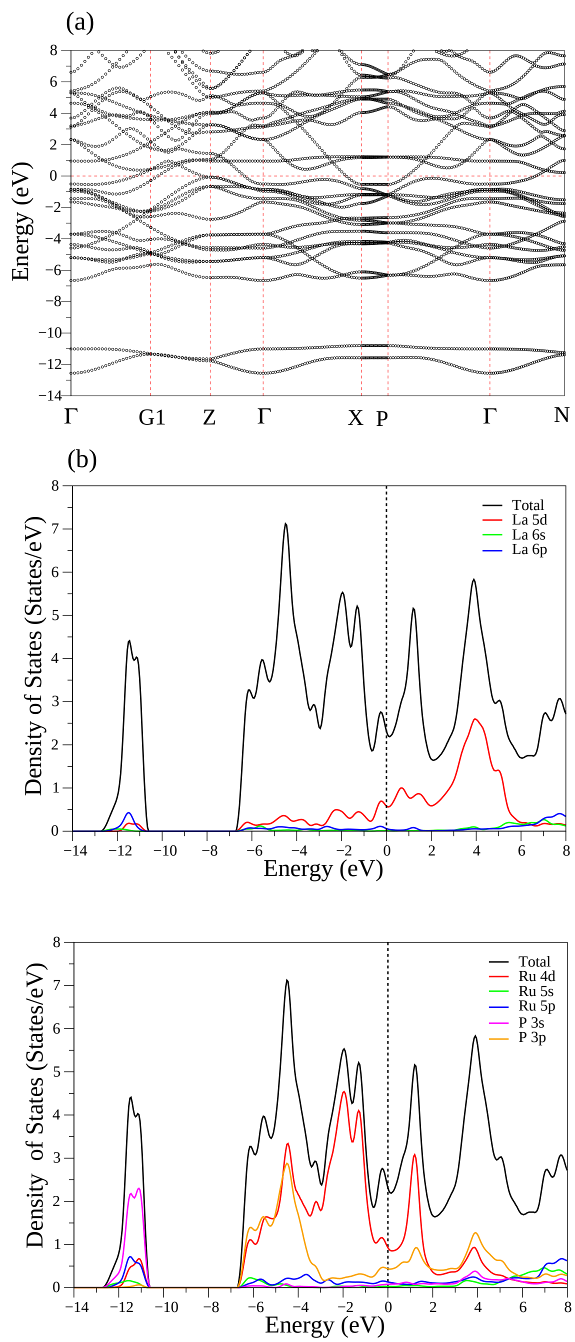

Figure 2. (a) The full electronic band structure for $LaRu_2P_2$ along selected symmetry lines in the Brillouin zone. (b) Total and partial electronic density of states (DOS). The Fermi level corresponds to 0 eV.

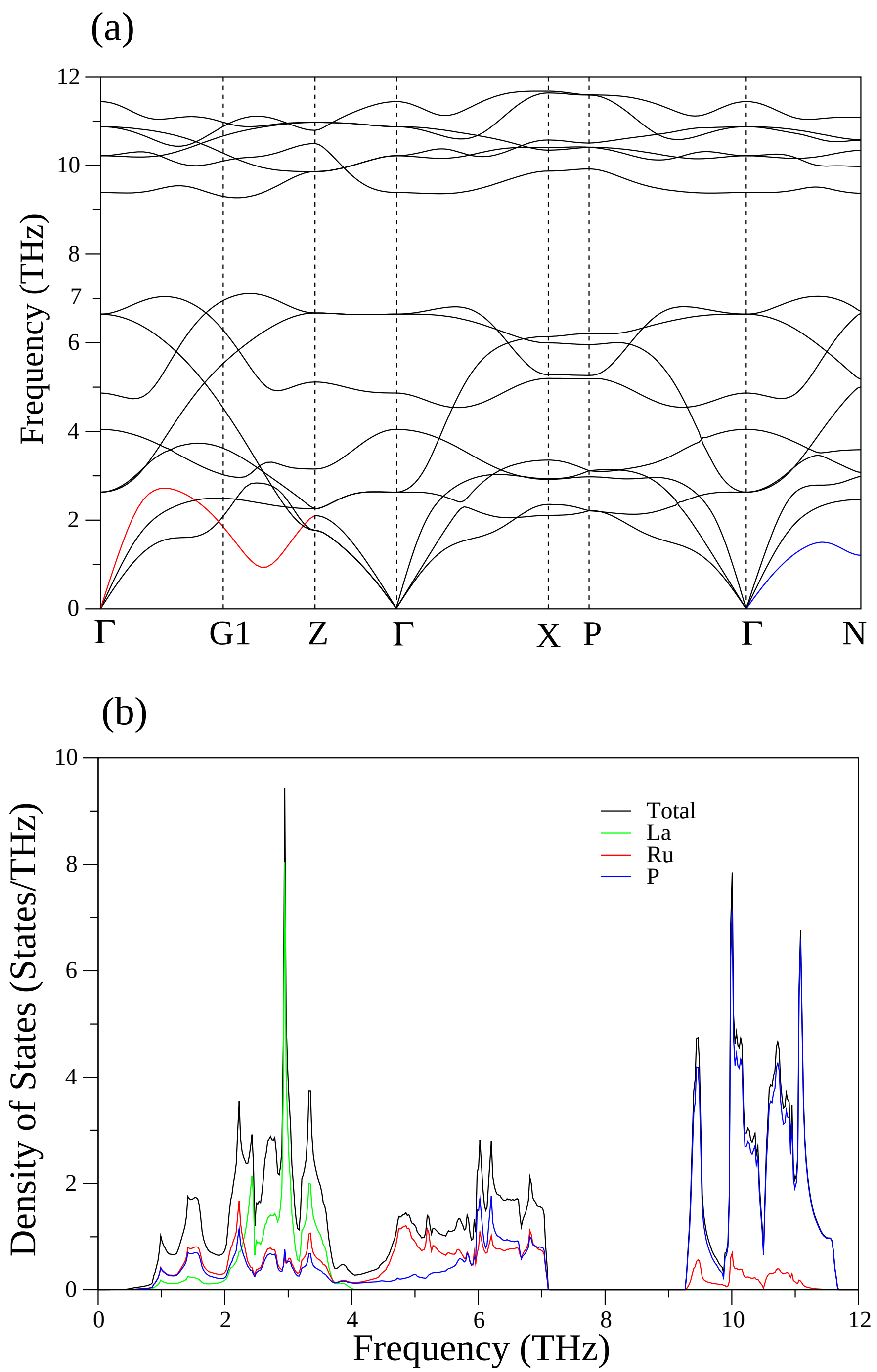

Figure 3. (a) The full phonon dispersion curves for $LaRu_2P_2$ along selected symmetry lines in the body-centered tetragonal zone. The anomaly of the longitudinal acoustic branch (LA) is shown by the red solid line and the anomaly of the lower-lying transverse acoustic branch (TA_1) is shown by the blue solid line . (b) Total and partial phonon density of states (DOS).

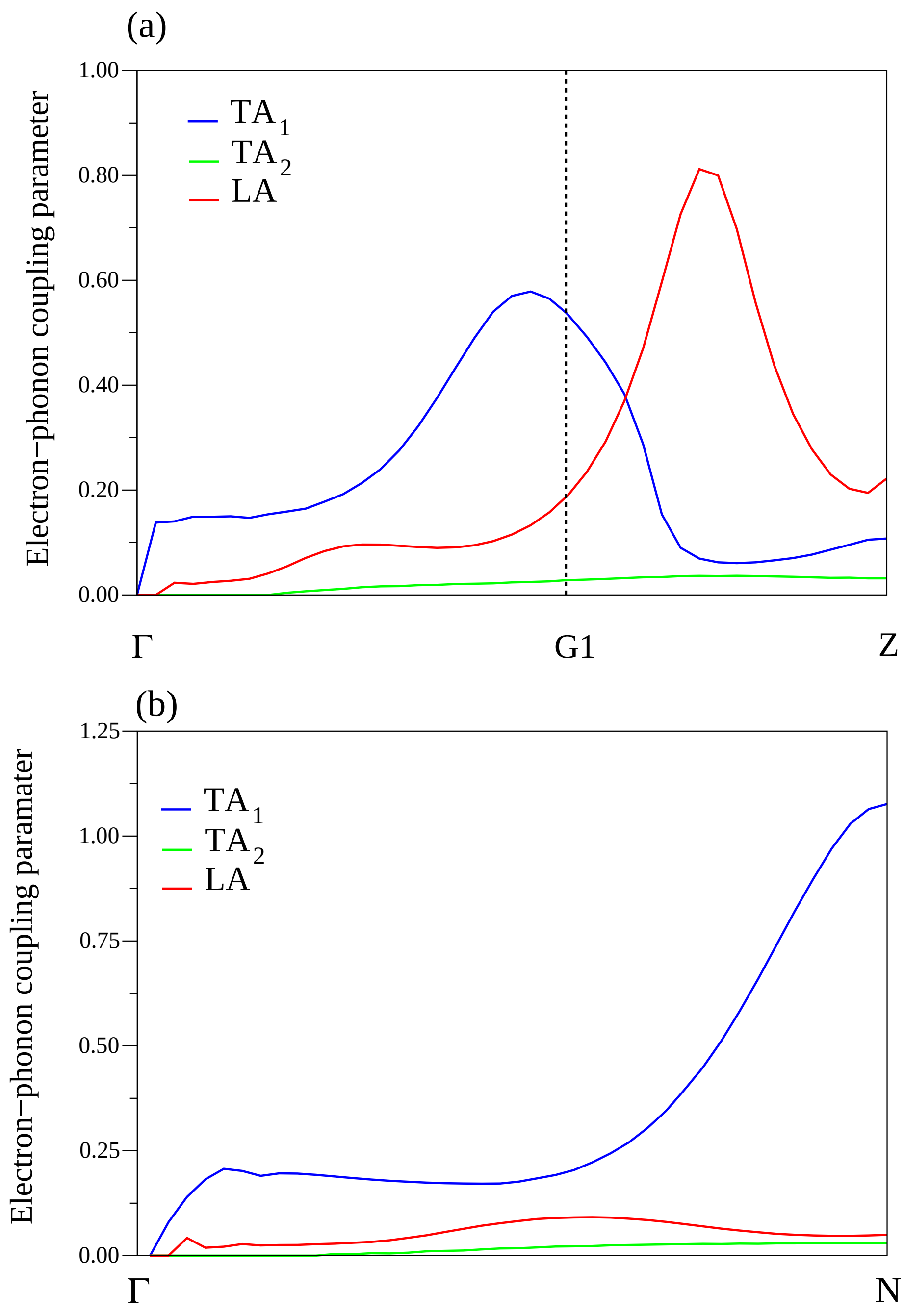

Figure 4. (a) The calculated wavevector-dependent electron-phonon coupling parameter for the acoustic branches along the Γ-G1-Z direction in the Brillouin zone. The Γ-G1 direction is the [100] direction. (b) The calculated wavevector-dependent electron-phonon coupling parameter for the acoustic phonon branches along the Γ-N direction in the Brillouin zone.

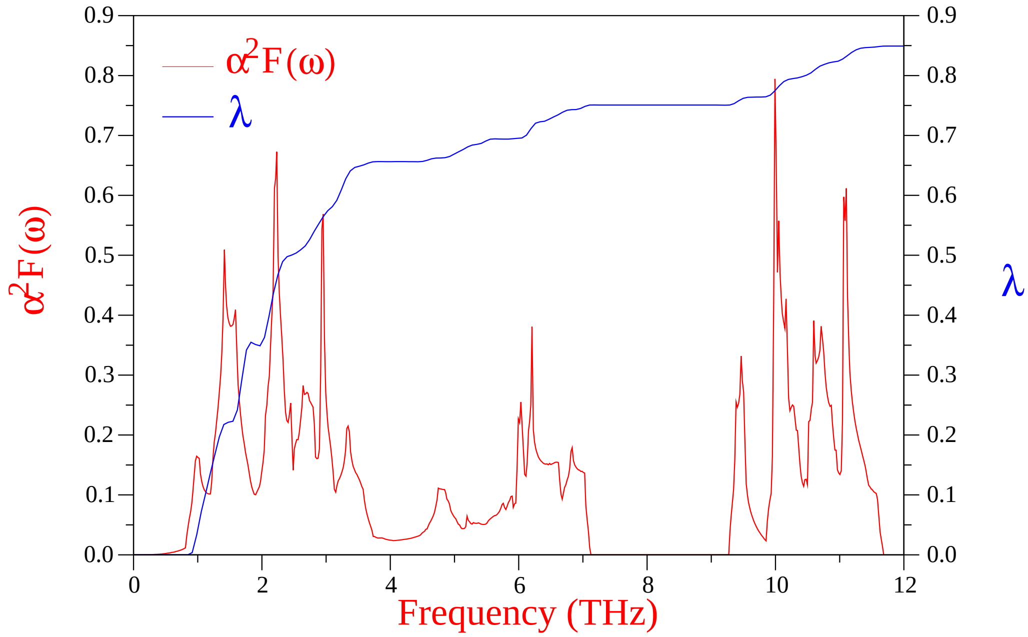

Figure 5. The calculated electron-phonon spectral function $\alpha^2F(\omega)$ (red line) and the frequency-accumulated electron-phonon coupling parameter $\lambda(\omega)$ (blue line) for $LaRu_2P_2$.

Table 1. Structural parameters for the body-centered tetragonal $LaRu_2P_2$, and their comparison with previous experimental and theoretical results. The α, β and γ angles are good indicators of distortion in the RuP_4 tetrahedron (see Fig. 1).

Source	$a(\AA)$	$c(\AA)$	z	B(GPa)	B'	$d_{Ru-P}(\AA)$	α	β	γ
This work	4.067	10.703	0.359	78.20	1.00	2.344	120.37^o	104.31^o	75.69^o
Experimental [2]	4.031	10.675	0.359			2.329	119.87^o	104.31^o	75.47^o
Experimental [22]	4.032	10.632							
Experimental [24]	4.025	10.662							
Theoretical [25]			0.362						

Table 2. Calculated zone-center phonon modes, their electron-phonon coupling parameters and their eigen characters for the body-centered tetragonal $LaRu_2P_2$.

Mode	E_u	A_{2u}	B_{1g}	E_g	A_{2u}	E_u	E_g	A_{1g}
ν (in THz)	2.662	4.052	4.866	6.646	9.394	10.217	10.876	11.443
λ	0.0143	0.047	0.066	0.048	0.007	0.006	0.015	0.075
Eigen characters	La+Ru+P	La+Ru+P	Ru	P+Ru	P+Ru	P+Ru	P+Ru	P

Table 3. The calculated superconducting state parameters for $LaRu_2P_2$. The calculated results are also compared with previous experimental and theoretical values.

Source	$N(E_F)$(States/eV)	μ^*	ω_{ln}(K)	λ	T_c(K)	$\gamma(\frac{mJ}{molK^2})$
This work	2.38	0.18	127.74	0.85	3.74	10.35
GGA [24]	2.46					
Experimental [2]				0.98	4.0	
Experimental [24]				0.98		11.50